



Review

Polyoxometalates Impact as Anticancer Agents

Fátima Carvalho ¹ and Manuel Aureliano ^{2,3,*}

¹ Faculdade de Medicina e Ciências Biomédicas (FMCB), Universidade do Algarve, Campus de Gambelas, 8005-139 Faro, Portugal

² Faculdade de Ciências e Tecnologia (FCT), Universidade do Algarve, 8005-139 Faro, Portugal

³ Centro de Ciências do Mar (CCMar), Universidade do Algarve, 8005-139 Faro, Portugal

* Correspondence: maalves@ualg.pt; Tel.: +351-289-900-805

Abstract: Polyoxometalates (POMs) are oxoanions of transition metal ions, such as V, Mo, W, Nb, and Pd, forming a variety of structures with a wide range of applications. Herein, we analyzed recent studies on the effects of polyoxometalates as anticancer agents, particularly their effects on the cell cycle. To this end, a literature search was carried out between March and June 2022, using the keywords “polyoxometalates” and “cell cycle”. The effects of POMs on selected cell lines can be diverse, such as their effects in the cell cycle, protein expression, mitochondrial effects, reactive oxygen species (ROS) production, cell death and cell viability. The present study focused on cell viability and cell cycle arrest. Cell viability was analyzed by dividing the POMs into sections according to the constituent compound, namely polyoxovanadates (POVs), polyoxomolybdates (POMos), polyoxopaladates (POPds) and polyoxotungstates (POTs). When comparing and sorting the IC₅₀ values in ascending order, we obtained first POVs, then POTs, POPds and, finally, POMos. When comparing clinically approved drugs and POMs, better results of POMs in relation to drugs were observed in many cases, since the dose required to have an inhibitory concentration of 50% is 2 to 200 times less, depending on the POMs, highlighting that these compounds could become in the future an alternative to existing drugs in cancer therapy.

Keywords: polyoxometalates; polyoxovanadates; polyoxotungstates; cell viability; cell cycle; drugs; cancer



Citation: Carvalho, F.; Aureliano, M. Polyoxometalates Impact as Anticancer Agents. *Int. J. Mol. Sci.* **2023**, *24*, 5043. <https://doi.org/10.3390/ijms24055043>

Academic Editors: Alexey Nazarov and Claudia Sissi

Received: 1 February 2023

Revised: 24 February 2023

Accepted: 28 February 2023

Published: 6 March 2023



Copyright: © 2023 by the authors. Licensee MDPI, Basel, Switzerland. This article is an open access article distributed under the terms and conditions of the Creative Commons Attribution (CC BY) license (<https://creativecommons.org/licenses/by/4.0/>).

1. Introduction

The application of metals such as platinum (Pt), lithium (Li), tungsten (W), gold (Au), and vanadium (V), among others, within chemical species, complexes, compounds and/or nanoparticles in biology has been a rapidly growing branch of science [1–7]. Besides platinum compounds, bio-active metal-based complexes, clusters such as gold compounds and polyoxometalates (POMs), and metal-based nanoparticles have shown anticancer, antiviral, and antibacterial activities, among others [1–13].

Regarding biomedical applications, the number of articles on POMs has tripled in the last decade [10], as illustrated by the well-studied polyoxovanadates (POVs) [14–18]. In fact, POMs are known to target several proteins such as aquaporins and P-type ATPases [11,13], although many other proteins and/or enzymes involved in many biochemical processes have been proposed to be affected [14–19]. The isopolyoxovanadate decavanadate (V₁₀) is perhaps the most widely studied POV in biology, affecting several biochemical and cellular processes [14–32].

Polyoxometalates (POMs) are oxoanions of transition metal ions, such as V, Mo, W, Nb, and Pd, forming a variety of structures with a wide range of applications [10,12,15,16]. They may also include other elements in their structure such as P (phosphorus) or As (arsenic), among others, and may have one of the main metallic oxoanions absent and/or replaced by other metals, such as Co (cobalt) or Mn (manganese), resulting in versatile structures (Figure 1), which give them a wide variety of chemical and physical properties [21].

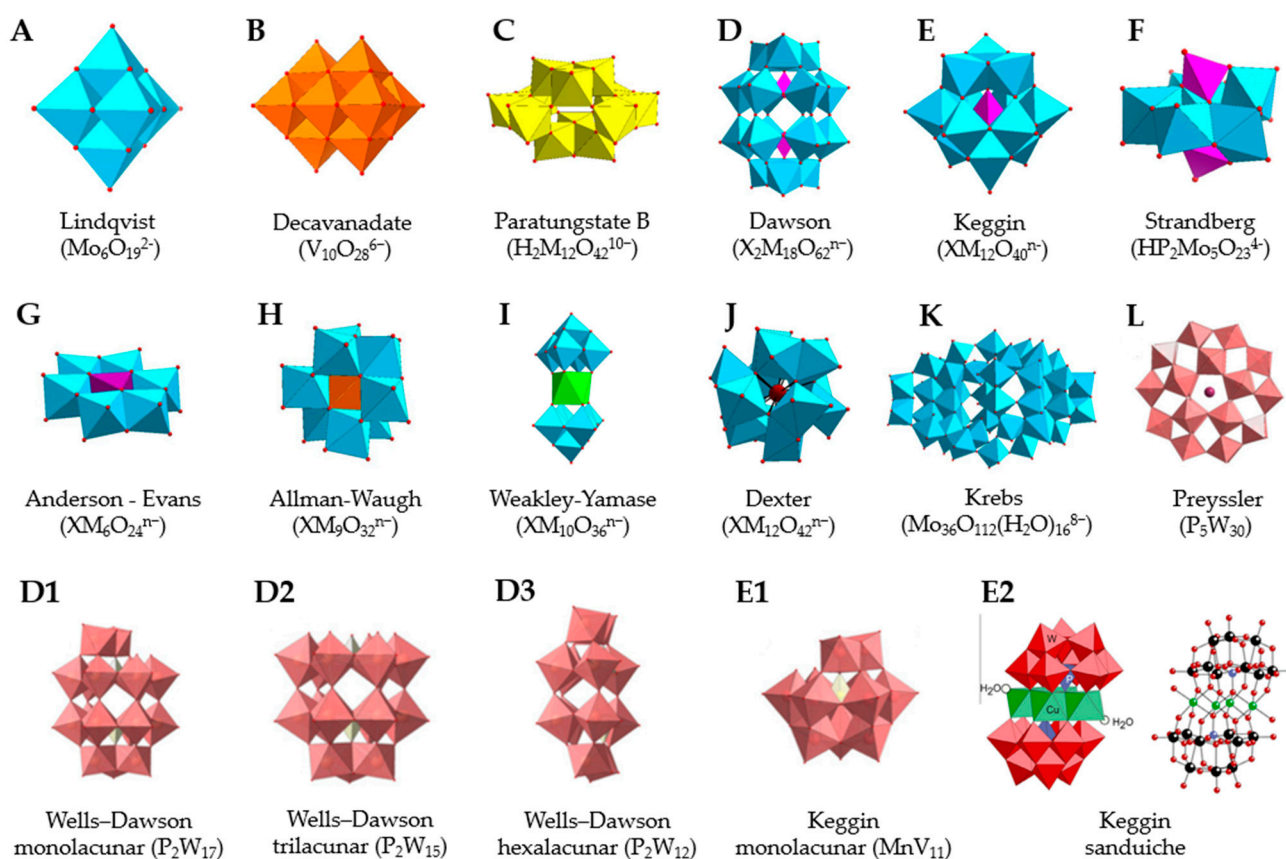


Figure 1. Examples of POM structures. (A)—Lindqvist ($\text{Mo}_6\text{O}_{19}^{2-}$); (B)—Isopolyoxometalate ($\text{V}_{10}\text{O}_{28}^{6-}$); (C)—Paratungstate B ($\text{H}_2\text{M}_{12}\text{O}_{42}^{10-}$); (D)—Dawson ($\text{X}_2\text{M}_{18}\text{O}_{62}^{n-}$); (E)—Keggin ($\text{XM}_{12}\text{O}_{40}^{n-}$); (F)—Strandberg ($\text{HP}_2\text{Mo}_5\text{O}_{23}^{4-}$); (G)—Anderson-Evans ($\text{XM}_6\text{O}_{24}^{n-}$); (H)—Allman-Waugh ($\text{XM}_9\text{O}_{32}^{n-}$); (I)—Weakley-Yamase ($\text{XM}_{10}\text{O}_{36}^{n-}$); (J)—Dexter ($\text{XM}_{12}\text{O}_{42}^{n-}$); (K)—Krebs ($\text{Mo}_{36}\text{O}_{112}(\text{H}_2\text{O})_{16}^{8-}$); (L)—Preyssler (P_5W_{30}) [21]. Lacunar POM-like structures, Dawson: (D1)—Wells-Dawson Monolacunar (P_2W_{17}) [21]; (D2)—Wells-Dawson trilacunar (P_2W_{15}) [21]; (D3)—Wells-Dawson hexalacunar (P_2W_{12}) [21] and Keggin type: (E1)—Keggin monolacunar (MnV_{11}) [21] and (E2)—Keggin sandwich [33]. Adapted with copyright permission from MDPI and Elsevier, respectively from references [21,33].

From the structure of a type of POM (polyoxometalate), such as Keggin or Dawson, (Figure 1D1–3,E1), it is possible to find lacunar derivatives, through the removal of one or more metal oxoanions. There are other compounds that can be formed from the structure of a type of Keggin POM, e.g., the sandwich type (Figure 1E2), which generally have two trilacunar anions separated by a belt of metallic cations.

In addition to the wide variety of chemical and physical properties, as mentioned before, this diversity of structures gives polyoxometalates numerous applications in several areas, such as environmental, chemical and industrial. Their effects are well known, mainly in catalysis, prevention of corrosion, and macromolecular crystallography, among others. Their usefulness in biomedicine [17,34,35] is also highlighted, namely through their antiviral [36–38] activity, where in the last two years, in the face of the world pandemic due to the SARS-CoV virus (severe acute respiratory syndrome coronavirus), studies have been carried out in an attempt to use POMs to help in fighting COVID-19 [39]. They are still useful in antitumor activities [40–44], and are antibacterial [16] and anti-inflammatory [45]. Additionally, they can also be used in biomedical engineering [46,47] in order to improve and develop innovative approaches to be applied in the prevention, diagnosis and therapy of diseases such as Alzheimer's [48–50] and diabetes [51], where

they tend to be demonstrated as potential drugs. In fact, the pharmacological action of POMs has sparked interest in them being potential candidates for therapeutic applications.

Since the beginning of the 21st century, and particularly recently, Aureliano's research group and collaborators have been publishing review papers, editorials, chapters and regular papers regarding metal complexes and/or POMs biological functions and their applications [10,15,16,18,19,21–23,26,52–56]. Herein, POMs biological effects were further highlighted as possible anticancer agents in the near future. Among these effects, even though studies are scarce and the mechanisms of action are unclear, the cell cycle is particularly focused on. Still, POMs may thus be used as a potential strategy in the future as antitumor drugs with specific actions, which suggest the blockage of various cellular mechanisms such as the cell cycle.

2. Results and Discussion

2.1. Types of POMs

Of the selected articles, 18 compounds were found under study, belonging to four types of POMs, depending on their fundamental compound: POVs (polyoxovanadates, polyoxometalates containing vanadium); those containing molybdenum (POMos, polyoxomolybdates); the POMs containing palladium (POPds, polyoxopaladates); and finally those containing tungsten (POTs, polyoxotungstates).

Starting with the POVs it was found that: (1) compounds with the molecular formula $\text{Na}_4\text{Co}_6\text{V}_{10}\text{O}_{28}\cdot 18\text{H}_2\text{O}$ (abbreviation CoV_{10}), $\text{Na}_3(12\text{H}_2\text{O})\text{H}_3\text{V}_{10}\text{O}_{28}\cdot 2\text{H}_2\text{O}$ (abbreviation NaV_{10}) an isopolyoxometalate with a decavanadate (V_{10}) a well known type of structure [57]; (2) the POV with the formula $\text{K}_{12}[\text{V}_{18}\text{O}_{42}(\text{H}_2\text{O})]\cdot 6\text{H}_2\text{O}$ (abbreviation V_{18}) being a vanadium [58] with a Keggin structure; and (3) the compound $6\{\text{V}_5\text{O}_9\text{Cl}(\text{COO})_4\}$ (abbreviation VMOP-31) [59] with a Lindqvist's type of structure.

Following the molybdenum compounds, we found the compound with the molecular formula $\text{K}_2\text{Na}[\text{As}^{\text{III}}\text{Mo}_6\text{O}_{21}(\text{O}_2\text{CCH}_2\text{NH}_3)_3]\cdot 6\text{H}_2\text{O}$, also designated in the article by compound 1, in order to facilitate [60], better known as arsenomolybdate with an Anderson–Evans structure, involved in a silica nanosphere ($\text{K}_2\text{Na}[\text{As}^{\text{III}}\text{Mo}_6\text{O}_{21}(\text{O}_2\text{CCH}_2\text{NH}_3)_3]\cdot 6\text{H}_2\text{O}$ (abbreviation POM@SiO₂) [61]; $\text{K}_2\text{Na}_2[\gamma\text{-Mo}_8\text{O}_{26}(\text{O}_2\text{CCH}_2\text{NH}_3)_2]\cdot 6\text{H}_2\text{O}$, designated as compound 2, which are heteropolymolybdates [62]; with a Strandberg structure the $\{[4,4'\text{-H}_2\text{bpy}]_2\{[4,4'\text{-H}_2\text{bpy}]_2\{[\text{H}_2\text{P}_2\text{Mo}_5\text{O}_{23}]\}\cdot 5\text{H}_2\text{O}$ [63]; and finally, the $[(\text{Cu}(\text{pic})_2)_2(\text{Mo}_8\text{O}_{26})]\cdot 8\text{H}_2\text{O}$ [64].

There are also PONMs or polyoxopaladates, with the molecular formulas and respective abbreviations: $\text{Na}_8[\text{Pd}_{13}\text{As}_8\text{O}_{34}(\text{OH})_6]\cdot 42\text{H}_2\text{O}$ (abbreviation Pd_{13}), $\text{Na}_4[\text{SrPd}_{12}\text{O}_6(\text{OH})_3(\text{PhAsO}_3)_6(\text{OAc})_3]_2\text{NaOAc}\cdot 32\text{H}_2\text{O}$ (abbreviation SrPd_{12}), $\text{Na}_6[\text{Pd}_{13}(\text{PhAsO}_3)_8]\cdot 23\text{H}_2\text{O}$ (Pd_{13}L), $\text{Na}_{12}[\text{Sn}^{\text{IV}}\text{O}_8\text{Pd}_{12}(\text{PO}_4)_8]\cdot 43\text{H}_2\text{O}$ (abbreviation SnPd_{12}), $\text{Na}_{12}[\text{Pb}^{\text{IV}}\text{O}_8\text{Pd}_{12}(\text{PO}_4)_8]\cdot 38\text{H}_2\text{O}$ (abbreviation PbPd_{12}) [65].

Lastly, the POMs that have the compound tungsten (POTs). We started with $\text{K}_7\text{Na}_3[\text{Cu}_4(\text{H}_2\text{O})_2(\text{PW}_9\text{O}_{34})_2]20\text{H}_2\text{O}$ (abbreviation PW_9Cu) which has a Dawson structure [33]. Following a homochiral polyoxometalate $\{\text{CoSb}_6\text{O}_4(\text{H}_2\text{O})_3[\text{Co}(\text{hmta})\text{SbW}_8\text{O}_{31}]_3\}^{15-}$ (1, hmta = hexamethylenetetramine) [66]; a tri-organic germanotungstate polyoxometalate-tin-substitute [67] $\{(n\text{-Bu})\text{Sn}(\text{OH})_3\text{GeW}_9\text{O}_{34}\}^{4-}\cdot 26\text{H}_2\text{O}$ PAC-320 that has been shown to be an inhibitor of histone deacetylase (HDACi) [68] and has a Keggin structure. Finally, the POT $\{[\text{Na}(\text{H}_2\text{O})_4][\text{Na}_{0.7}\text{Ni}_{5.3}(\text{imi})_2(\text{Himi})(\text{H}_2\text{O})_2(\text{SbW}_9\text{O}_{33})_2]\} 10\text{H}_2\text{O}$, designated as compound 1 and $\text{H}_3[(\text{CH}_3)_4\text{N}]_4[\text{Na}_{0.7}\text{Co}_{5.3}(\text{imi})_2(\text{Himi})(\text{H}_2\text{O})_2(\text{SbW}_9\text{O}_{33})_2] 12\text{H}_2\text{O}$, also known as compound 2 [67], whose structure is a hybrid Keggin sandwich.

The 18 compounds are represented below, in the form of a table, with the division of the POMs by main component and in the order in which they appear in the periodic table, i.e., vanadium (V); molybdenum (Mo); palladium (Pd) and tungsten (W), according to their increasing atomic number, as presented above. Each compound is presented in Table 1 with its designation, that is, its molecular formula or abbreviation when existing; the structure with the respective illustration; the type of structure; bibliographic reference and POM of the 13 selected articles (Table 1).

Table 1. Representation of the formula, structure and type of the POMs referred to in the selected articles.

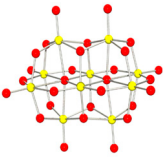
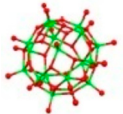
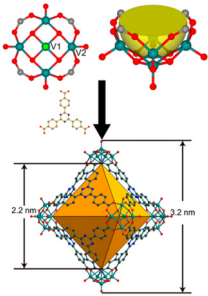
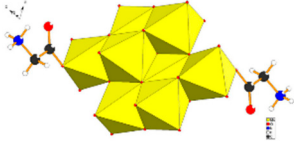
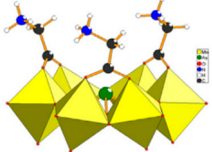
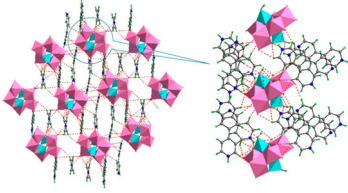
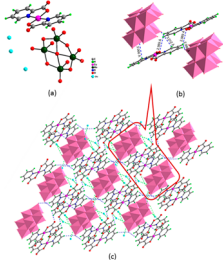
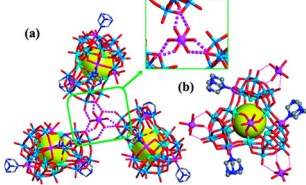
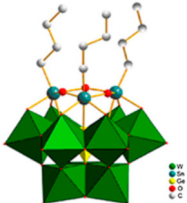
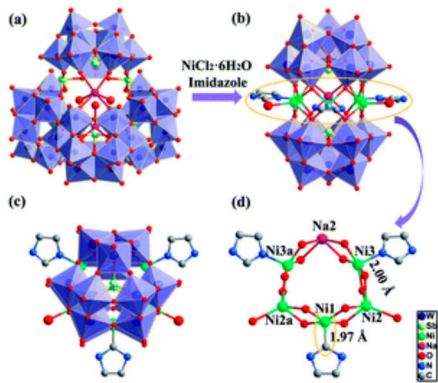
POM Formula (Abbreviation)	Structure	Structure Type	Ref.
POVs			
$\text{Na}_4\text{Co}_6\text{V}_{10}\text{O}_{28}\cdot 18\text{H}_2\text{O}$ (CoV ₁₀) $\text{Na}_3(12\text{H}_2\text{O})\text{H}_3\text{V}_{10}\text{O}_{28}\cdot 2\text{H}_2\text{O}$ (NaV ₁₀)		Decavanadate	[23,57]
$\text{K}_{12}[\text{V}_{18}\text{O}_{42}(\text{H}_2\text{O})] \cdot 6\text{H}_2\text{O}$ (V ₁₈)		Keggin	[58]
$6\{\text{V}_5\text{O}_9\text{Cl}(\text{COO})_4\}$ (VMOP-31)		Lindqvist	[59]
POMos			
$\text{K}_2\text{Na}[\text{As}^{\text{III}}\text{Mo}_6\text{O}_{21}(\text{O}_2\text{CCH}_2\text{NH}_3)_3]$ $6\text{H}_2\text{O}$ —(compound 1)		Anderson–Evans	[62]
$\text{K}_2\text{Na}_2[\gamma\text{-Mo}_8\text{O}_{26}(\text{O}_2\text{CCH}_2\text{NH}_3)_2]$ $6\text{H}_2\text{O}$ —(compound 2)			
$[[4,4'\text{-H}_2\text{bpy}]\{4,4'\text{-Hbpy}\}_2\{\text{H}_2\text{P}_2\text{Mo}_5\text{O}_{23}\}]\cdot 5\text{H}_2\text{O}$		Strandberg	[63]
$[(\text{Cu}(\text{pic})_2)_2(\text{Mo}_8\text{O}_{26})]\cdot 8\text{H}_2\text{O}$		Anderson–Evans	[64]

Table 1. Cont.

POM Formula (Abbreviation)	Structure	Structure Type	Ref.
$K_2Na[As^{III}Mo_6O_{21}(O_2CCH_2NH_3)_3] \cdot 6H_2O$ (POM@SiO ₂)		Anderson–Evans	[61,62]
$K_2Na[As^{III}Mo_6O_{21}(O_2CCH_2NH_3)_3] \cdot 6H_2O$		Anderson–Evans	[60,62]
POPds			
$Na_8[Pd_{13}As_8O_{34}(OH)_6] \cdot 42H_2O$ (Pd ₁₃)			
$Na_4[SrPd_{12}O_6(OH)_3(PhAsO_3)_6(OAc)_3] \cdot 2NaOAc \cdot 32H_2O$ (SrPd ₁₂)			
$Na_6[Pd_{13}(PhAsO_3)_8] \cdot 23H_2O$ (Pd ₁₃ L)		Unidentified	[65]
$Na_{12}[Sn^{IV}O_8Pd_{12}(PO_4)_8] \cdot 43H_2O$ (SnPd ₁₂)			
$Na_{12}[Pb^{IV}O_8Pd_{12}(PO_4)_8] \cdot 38H_2O$ (PbPd ₁₂)			
POTs			
$K_7Na_3[Cu_4(H_2O)_2(PW_9O_{34})_2]20H_2O$ (PW ₉ Cu)		Keggin sandwich	[33]

Table 1. Cont.

POM Formula (Abbreviation)	Structure	Structure Type	Ref.
$\{\text{CoSb}_6\text{O}_4(\text{H}_2\text{O})_3[\text{Co}(\text{hmta})\text{SbW}_8\text{O}_{31}]_3\}^{15}$		Homochiral	[66]
$\{(\text{n-Bu})\text{Sn}(\text{OH})\}_3\text{GeW}_9\text{O}_{34}]^{4-} \cdot 26\text{H}_2\text{O}$ (PAC-320)		Keggin	[68,69]
$\text{H}_2[(\text{CH}_3)_4\text{N}]^{4-}$ $\{[\text{Na}(\text{H}_2\text{O})_4][\text{Na}_{0.7}\text{Ni}_{5.3}(\text{imi})_2(\text{Himi})$ $(\text{H}_2\text{O})_2(\text{SbW}_9\text{O}_{33})_2]\} 10\text{H}_2\text{O}$ ($\text{C}_{25}\text{N}_{10}\text{Na}_{1.7}\text{Ni}_{5.3}\text{O}_{82}\text{Sb}_2\text{W}_{18}$) $\text{H}_3[(\text{CH}_3)_4\text{N}]_4[\text{Na}_{0.7}\text{Co}_{5.3}(\text{imi})_2(\text{Himi})$ $(\text{H}_2\text{O})_2(\text{SbW}_9\text{O}_{33})_2]\} 12\text{H}_2\text{O}$ ($\text{C}_{25}\text{N}_{10}\text{Na}_{0.7}\text{Co}_{5.3}\text{O}_{76}\text{Sb}_2\text{W}_{18}$)		Keggin sandwich	[67]

2.2. Types of Cancers

In these articles, several types of cancer were studied, and sometimes an article analyzed more than one type of cancer. These were namely gastric, colon, liver, lung, ovary, breast, prostate, leukemia, osteosarcoma, neuroblastoma and human hepatocellular carcinoma (Figure 2).

Through the analysis of Figure 2, it can be observed that the most studied types of cancer were lung and breast cancer, with six articles each, followed by liver cancer, covered in four articles.

2.3. POMs Effects

In the 13 articles, various effects of the selected POMs were analyzed, such as protein expression, mitochondrial effects, reactive oxygen species (ROS) production, cell cycle arrest, cell death, cell viability and anticancer activity, in vivo, or the antibacterial activity (Figure 3).

As seen in Figure 3, not all articles addressed all the effects of POMs, and there were effects addressed only in one article, such as antibacterial activity, analyzed in *Escherichia coli* (*E. coli*) regarding the effects of $[(\text{Cu}(\text{pic})_2)_2(\text{Mo}_8\text{O}_{26})] \cdot 8\text{H}_2\text{O}$, where it was shown to be quite effective with a minimum inhibitory concentration of approximately 135 $\mu\text{g}/\text{mL}$, which is the lowest value reported so far for any octamolybdate-based POM [64]. ROS production was also analyzed, as well as mitochondrial effects and protein expression in two, three and eight articles, respectively (Figure 3).

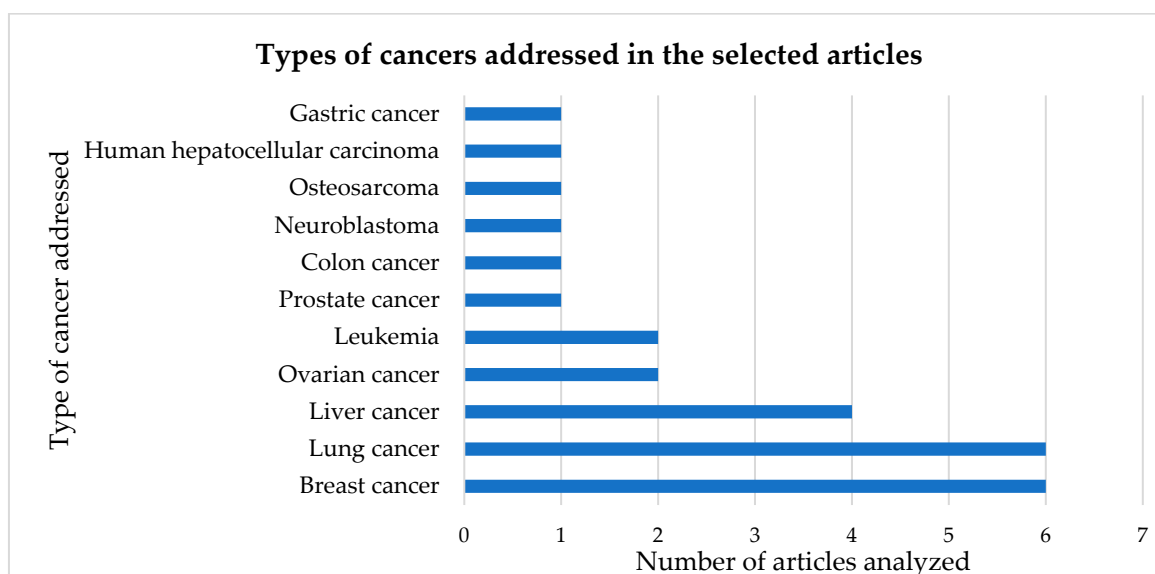


Figure 2. Number of articles for the different types of cancers studied.

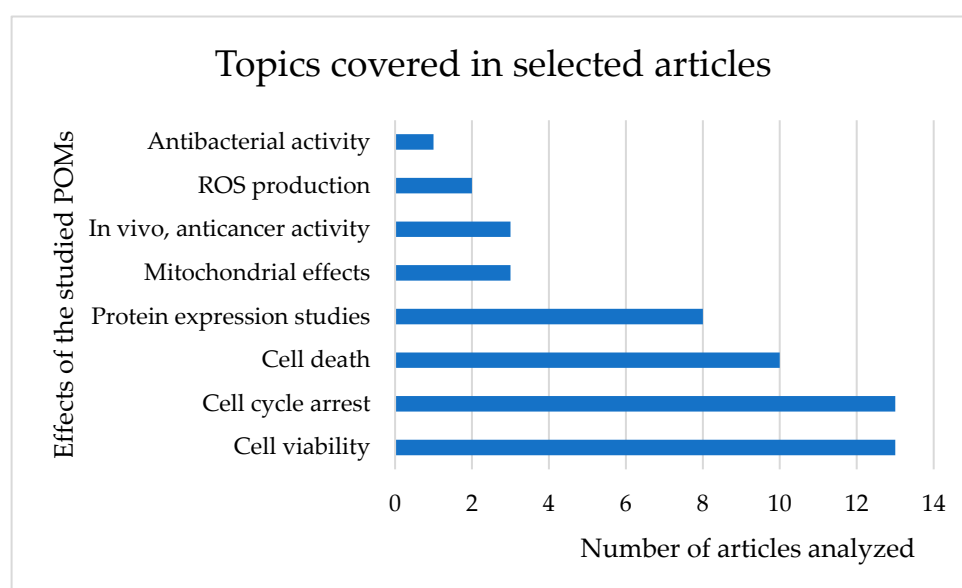


Figure 3. Number of articles in which each effect of the selected POMs was analyzed.

The production of ROS was verified in two articles, one of them with compounds containing noble metals (PONMs) [65]. The determination of the levels of superoxide ion produced was verified after 2 and 4 h of treatment. For this purpose, the dihydroethidium (DHE) method was used to detect cytosolic O_2^- , which is not fluorescent but, being oxidized to $O_2^{\cdot-}$, emits fluorescence. Through the method presented above, it was observed that the polyoxopalladate Pd_{13} induced about 30% of increased production of superoxide ion ($O_2^{\cdot-}$) at 4h after treatment. Furthermore, the polyoxopalladates Pd_{13} , $SnPd_{12}$ and $PbPd_{12}$ induced oxidative stress of HL-60 cells (human leukemia cells) resulting in an increase in the total production of reactive oxygen species [65].

Among the three articles selected for those that studied mitochondrial effects, the present study focused on the use of PAC-320. It was observed that with its use, in DU145 cells (human prostate tumor cells) there was a loss of MMP (mitochondrial membrane potential— $\Delta\Psi_m$). Consequently, cytochrome c is released in the cytosol, stimulating caspases that are associated apoptosis. Hence, it was deduced that apoptotic cell death was caused by the mitochondria-mediated pathway [68]. The same compound discussed above

was one of the eight that referred to the study of protein expression. PAC-320 also inhibits the enzymatic activity of HDAC (histone deacetylases) 1, 2, 4, 5 and 6, but to a lesser extent HDAC 3 [68].

Only three articles performed in vivo studies in order to confirm or refute the anti-cancer activity of POMs. Of these three studies, *Mus musculus* (mice) were selected as an animal model. In one of these articles, nude mice with DU145 lineage (human prostate cancer cell line) were selected [68]. After this, these mice were divided into groups where each group was injected with a different compound. One group received a solution containing the compound PAC-320 (50 mg/kg) and another NaB (sodium butyrate) (1 g/kg). Others received SAHA (suberoylanilide acid, Vorinostat, an HDACi inhibitor, which was approved in October 2006 by the US Food and Drug Administration (FDA) for the treatment of cutaneous manifestations of T-cell lymphoma (CTCL) in patients with progressive, persistent or recurrent disease after two systemic therapies) [70], with a concentration of 40 mg/kg. All groups were injected daily for 16 days [68].

Through the results obtained, it was observed that the group treated with PAC-320 did not show a noticeable effect on body weight. In this group, the inhibition of the growth of prostate tumors was on average 69.2% compared to the control, treated with the vehicle alone (DMSO), while treatment with the drug SAHA or the compound NaB was inhibited by 55.5% and 64.2%, respectively. The weight of the tumors was reduced on the 17th day, when they were dissected [68]. To our knowledge, the precise mechanism of action responsible for the prostate tumor inhibition is yet to be clarified. In fact, although several putative mechanisms against cancer were recently reviewed [10,15,18], how the POM chemistry is specifically affecting the growth inhibition of prostate tumors needs further understanding.

In another study, over 12 consecutive days, mice with H22 liver tumor (Hepatoma-22, mouse liver tumor cell line) were administered treatments intraperitoneally, one with a saline solution (negative control group); cisplatin (CDDP or cis-diaminodichloroplatinum or cis-Pt) was used as the positive control group at a dose of 3 mg/kg. CDDP is a well-known platinum-based chemotherapy drug that is used to treat many types of cancer, including sarcomas, some carcinomas (e.g., small cell lung cancer and ovary cancer), lymphomas and germ cell tumors. Others received the studied compound, VMOP-31, at a dose of 12.5, 25 and 50 mg/kg [59]. On the 14th day, when they were excised, VMOP-31 led to a decrease in tumor weight compared to the saline group, but similar to that of the cisplatin group. Tumor inhibition rates of VMOP-31 at doses of 12.5, 25 and 50 mg/kg were determined to be 32.7, 39.6 and 56.4%, respectively [59]. Cisplatin has a tumor inhibition rate of 58.4%, which is comparable to the VMOP-31 tumor inhibition rate at 50 mg/kg. In this study, it was also observed that the body weight of the mice increased continuously, except for those in the cisplatin group, where the weight decreased continuously, which indicates that cisplatin has side effects [59].

Finally, we identified a study where 10 mice were randomly assigned and injected with mouse liver tumor cells (Hep-A-22) on their backs [57]. After 7 days of tumor cell administration, the mice were treated by intraperitoneal injections of CoV₁₀ solutions with increasing concentrations (2, 6 and 12 mg/kg) [57], which were continued for 14 days. On the other hand, control mice were treated with saline solution for 2 weeks, under the same conditions that were used for animals treated with the CoV₁₀ compound. As a result, it was observed that the average tumor weight with a concentration of 2 mg/kg with the CoV₁₀ solution was 1.750 g [57], about 1.40-times lower than the average weight of the control group (2.440 g). As for the control group, compared with the value obtained (1.490 g) at a concentration of 12 mg/kg, a value about 1.6-times lower was observed. Comparing the control to a dose of 20 mg/kg of the approved drug, 5-Fu (fluorouracil is a widely used medicine in oncology, being therefore a base for a large part of current chemotherapy regimens to treat a wide spectrum of cancers), the mean tumor weight value was 0.477 g, i.e., 5.1-times lower. Note that here the dose used is higher than the dose used with the POM. Perhaps the higher dose of the drug justifies it being more harmful in reducing the

weight of the mice, proving to be more toxic [57]. Furthermore, from the animal body weight data, it was found that CoV₁₀ could decrease body weight less than the 5-Fu dose, thus showing less toxicity. It can also be seen that the inhibiting effect of the medium dose is better than that of the higher dosage (12 mg/kg). The reason may be that higher dosages of CoV₁₀ can affect the function of immune organs, leading to decreased immune capacity [57].

However, several studies demonstrate that the oral administration of POMs is presumed safe and poses a low risk of potential health risks. Furthermore, for potential antidiabetic POTs it was concluded that the hepatotoxic and nephrotoxic effects could be considered as mild. Thus, besides POMs presenting higher antitumor activity and lower toxicity in in vitro and in vivo experiments, they have also been described as promising agents in the treatment of infectious diseases, diabetes and Alzheimer's disease [69,71–73].

2.3.1. Cell Viability

As discussed above, it was found that 13 articles analyzed cell death and that all selected articles refer to the effects of POMs on cell viability, and where cell cycle arrest was given (Figure 3). In these articles, the IC₅₀ values (POM concentration that inhibits 50% of cell viability) of the various POMs selected in each article in the respective cell lines studied were analyzed. To understand which POM had the lowest IC₅₀, a comparison was made, through a table containing the IC₅₀ of the various compounds and the strains in which each one was applied, after exposure of 24, 48 and 72 h to POVs, POMos, POPds and POTs. The cell lines within each division were ordered alphabetically from A–Z (Table 2).

Table 2. IC₅₀ values (μM) of the different POMs studied in the respective cell lines.

Formula or Abbreviation	Cell Line	IC ₅₀ (μM)			Ref.
		24 h	48 h	72 h	
POVs					
VMOP-31	A549	2.64	0.74	0.55	[59]
	BEAS-2B	15.46	3.13	1.84	
	HL-60	14.66	2.04	1.61	
V ₁₈	MCF-7	45.95	11.95	12.49	[58]
VMOP-31	MCF-7	1.52	0.63	0.53	[59]
V ₁₈	MDA-MB-231	>500	360.32	135.66	[58]
CoV ₁₀	SK-OV-3			<0.24 *	[57]
NaV ₁₀	SK-OV-3			18.90 *	
Co(Ac) ₂	SK-OV-3			50.90 *	
CoV ₁₀	SMMC-7721			<0.26 *	
NaV ₁₀	SMMC-7721			9.56 *	
Co(Ac) ₂	SMMC-7721			44.90 *	
VMOP-31	SMMC-7721	2.66	1.17	0.75	[59]
POMos					
K ₂ Na[As ^{III} Mo ₆ O ₂₁ (O ₂ CCH ₂ NH ₃) ₃] 6H ₂ O	A549	332.87		180.40	[62]
K ₂ Na ₂ [γ-Mo ₈ O ₂₆ (O ₂ CCH ₂ NH ₃) ₂]	A549	1072.02		330.18	
[[4,4'-H ₂ bpy]{4,4'-Hbpy} ₂ {H ₂ P ₂ Mo ₅ O ₂₃ }] ₂ ·5H ₂ O	4549	25.17			[63]
[(Cu(pic) ₂) ₂ (Mo ₈ O ₂₆)] 8H ₂ O	A549		25.00		[64]

Table 2. Cont.

Formula or Abbreviation	Cell Line	IC ₅₀ (μM)			Ref.
		24 h	48 h	72 h	
[[4,4'-H ₂ bpy]{4,4'-Hbpy} ₂ {H ₂ P ₂ Mo ₅ O ₂₃ }]·5H ₂ O	HepG2	33.79			[63]
[(Cu(pic) ₂) ₂ (Mo ₈ O ₂₆)]·8H ₂ O	HepG2		21.56		[64]
K ₂ Na[As ^{III} Mo ₆ O ₂₁ (O ₂ CCH ₂ NH ₃) ₃]·6H ₂ O	HL-60	8.61	0.13	19.49	[60]
	HUVEC	889.18			
K ₂ Na[As ^{III} Mo ₆ O ₂₁ (O ₂ CCH ₂ NH ₃) ₃]·6H ₂ O (POM@SiO ₂)	MCF-7	40.00 *	10.80 *	1.70 *	[61]
[[4,4'-H ₂ bpy]{4,4'-Hbpy} ₂ {H ₂ P ₂ Mo ₅ O ₂₃ }]·5H ₂ O	MCF-7	32.11			[63]
[(Cu(pic) ₂) ₂ (Mo ₈ O ₂₆)]·8H ₂ O	MCF-7		24.24		[64]
K ₂ Na[As ^{III} Mo ₆ O ₂₁ (O ₂ CCH ₂ NH ₃) ₃]·6H ₂ O	U937	14.50	5.65	2.73	[60]
POPds					
PbPd ₁₂	SH-SY5Y	>>100	>>100		[65]
Pd ₁₃	SH-SY5Y	7.20	4.40		
Pd ₁₃ L	SH-SY5Y	63.80	21.40		
SnPd ₁₂	SH-SY5Y	>>100	>>100		
SrPd ₁₂	SH-SY5Y	75.80	76.70		
POTs					
[Co(H ₂ O) ₆ {CoSb ₆ O ₄ (H ₂ O) ₃ {Co(hmta)SbW ₈ O ₃₁ }] ₃] ¹³⁻	A2780			0.77	[66]
{Sb ₉ W ₂₁ }	A2780			4.44	
[Co(H ₂ O) ₆ {CoSb ₆ O ₄ (H ₂ O) ₃ {Co(hmta)SbW ₈ O ₃₁ }] ₃] ¹³⁻	A2780cis			4.35	[66]
{Sb ₉ W ₂₁ }	A2780cis			29.02	
[Co(H ₂ O) ₆ {CoSb ₆ O ₄ (H ₂ O) ₃ {Co(hmta)SbW ₈ O ₃₁ }] ₃] ¹³⁻	A549			12.65	[67]
C ₂₅ N ₁₀ Na _{1.7} Ni _{5.3} O ₈₂ Sb ₂ W ₁₈	A549		39.75		
C ₂₅ N ₁₀ Na _{1.7} Ni _{5.3} O ₈₂ Sb ₂ W ₁₈	AGS		1.75		
C ₂₅ N ₁₀ Na _{0.7} Ni _{5.3} O ₇₆ Sb ₂ W ₁₈	AGS		1.42		
{Sb ₈ W ₃₆ }	AGS		2.86		
{SbW ₉ }	AGS		26.22		
C ₂₅ N ₁₀ Na _{1.7} Ni _{5.3} O ₈₂ Sb ₂ W ₁₈	BGC-823		22.27		
C ₂₅ N ₁₀ Na _{0.7} Ni _{5.3} O ₇₆ Sb ₂ W ₁₈	BGC-823		20.51		
{Sb ₈ W ₃₆ }	BGC-823		8.68		
{SbW ₉ }	BGC-823		188.28		
[Co(H ₂ O) ₆ {CoSb ₆ O ₄ (H ₂ O) ₃ {Co(hmta)SbW ₈ O ₃₁ }] ₃] ¹³⁻	CT26			14.72	[66]
PAC-320	DU145			4.55	[68]
[Co(H ₂ O) ₆ {CoSb ₆ O ₄ (H ₂ O) ₃ {Co(hmta)SbW ₈ O ₃₁ }] ₃] ¹³⁻	HT29			15.60	[66]
C ₂₅ N ₁₀ Na _{1.7} Ni _{5.3} O ₈₂ Sb ₂ W ₁₈	H1299		63.23		[67]
C ₂₅ N ₁₀ Na _{1.7} Ni _{5.3} O ₈₂ Sb ₂ W ₁₈	HEK293T		114.76		
C ₂₅ N ₁₀ Na _{0.7} Ni _{5.3} O ₇₆ Sb ₂ W ₁₈	HEK293T		103.09		
C ₂₅ N ₁₀ Na _{1.7} Ni _{5.3} O ₈₂ Sb ₂ W ₁₈	HepG2		42.98		
PAC-320	LNCaP			5.64	[68]
PW ₉ Cu	MC3T3-E1	92.00			[33]
[Co(H ₂ O) ₆ {CoSb ₆ O ₄ (H ₂ O) ₃ {Co(hmta)SbW ₈ O ₃₁ }] ₃] ¹³⁻	MCF-7			12.24	[66]

Table 2. Cont.

Formula or Abbreviation	Cell Line	IC ₅₀ (μM)			Ref.
		24 h	48 h	72 h	
PW ₉ Cu	MG-63	22.00			[33]
[Co(H ₂ O) ₆ {CoSb ₆ O ₄ (H ₂ O) ₃ [Co(hmta)SbW ₈ O ₃₁] ₃ }] ¹³⁻	OVCAR-3			1.78	[66]
{Sb ₉ W ₂₁ }	OVCAR-3			8.80	[67]
[Co(H ₂ O) ₆ {CoSb ₆ O ₄ (H ₂ O) ₃ [Co(hmta)SbW ₈ O ₃₁] ₃ }] ¹³⁻	SK-OV-3			15.02	[66]
C ₂₅ N ₁₀ Na _{1.7} Ni _{5.3} O ₈₂ Sb ₂ W ₁₈	SMMC-7721		48.29		[67]
PW ₉ Cu	UMR106	81.00			[33]

* Note: IC₅₀ values in the table marked with (*) are measured in μg/mL.

Five vanadium POMs were studied, from three POVs that were analyzed in eight cell lines (Table 2, Figure 4). Among these POVs, it was observed in the MCF-7 lineage (human breast cancer cell line) that the best IC₅₀ was 0.53 μM at 72 h, achieved with the POV VMOP-31 [59] and corresponding to the best value of the polyoxovanadates. When comparing this value to V₁₈ (45.95 μM) [58], in the same strain, whether at 24, 48 or 72 h, it always presents better results, being about 30 times (more potent) for 24 h. With CoV₁₀, the SMMC-7721 lineage (human papillomavirus-related endocervical adenocarcinoma cell line) resulted in a value of <0.26 μg/mL [57], which proved to be about 73- to 196-times more efficient than NaV₁₀ compounds (18.90 μg/mL) and Co(Ac)₂ (50.90 μg/mL) [57], such as in SK-OV-3 (human ovarian cancer cell line). For this strain, the best value is <0.24 μg/mL, when compared to the compounds NaV₁₀ (9.56 μg/mL) and Co(Ac)₂ (44.90 μg/mL), that is, CoV₁₀ [57] was about 40- to 187-times more efficient than these compounds. These values cannot be compared with those of other vanadium compounds, since the measurement units are not the same.

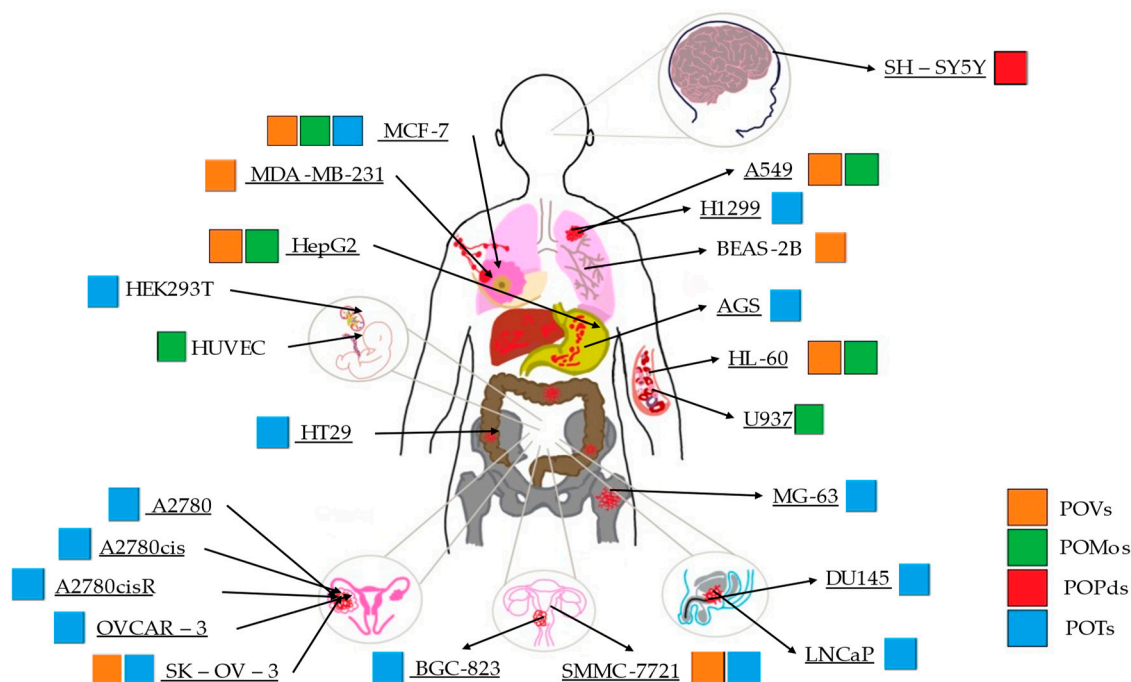


Figure 4. Illustration of the 23 human cell lines tested in the study of cell viability of different types of POMs. A total of 20 tumor lineages are underlined and 3 are not underlined, which are non-tumor cell lines. The color scheme is representative of each type of POM studied: POVs in orange, POMos in green, POPds in red and POTs in blue.

In polyoxometalates containing molybdenum, six compounds were analyzed in six cell lines (Figure 4). It is observed in Table 2 that the A549 line (human lung cancer cell line) showed the best IC₅₀ value to be 25 µM at 24 h, with the hybrid compound of structure Anderson–Evans (Figure 1G) and formula [(Cu(pic)₂)₂(Mo₈O₂₆)]·8H₂O (Table 1). This same compound also showed a similar value (21.56 µM) in the HepG2 lineage (Human liver cancer cell line) at 48 h. Furthermore, in breast cancer, this compound showed a similar inhibition potency (24.24 µM) [71]. In the MCF-7 lineage, the compound K₂Na[As^{III}Mo₆O₂₁(O₂CCH₂NH₃)₃]-6H₂O (POM@SiO₂) with the same structure as the previous one, but inserted in silica nanoparticles (see structure in Table 1), presented the best IC₅₀ value (1.70 µg/mL) at 72 h [61], however this cannot be compared, as they have different measurement units.

Of the five palladium-containing PONMs [65], all were studied in the same cell line SH-SY5Y (three times cloned subline from neuroblastoma cell line SK-N-SH (ATCC HTB-11)). It was verified that the PONM that showed a better value both at 24 and 48 h was Pd₁₃ (Table 1), with values of 7.20 and 4.40 µM, respectively, when compared to their hybrids containing phenyl groups (63.80 and 21.40 µM for Pd₁₃L, 75.80 and 76.70 µM for SrPd₁₂) [65], i.e., between 5 and 9 times for the first and between 11 and 17 times for the second, as the first was less efficient.

Regarding tungsten-containing compounds with effects on cell viability, eight compounds addressed in 15 different cell lines were found (Table 2, Figure 4). With POTs, in the A2780 and A2780cis lineage (human ovarian cancer cell line and the same lineage but resistant to cisplatin), the best values were obtained at 72 h with the compound [Co(H₂O)₆{CoSb₆O₄(H₂O)₃[Co(hmta)SbW₈O₃₁]₃}]¹³⁻ which presents a homochiral, sandwich-like structure (Table 1), and were, respectively, 0.77 and 4.35 µM [66]. This was 6-times more efficient in the non-resistant cell line when compared with lines resistant to cisplatin treatment. In the AGS lineage (human stomach cancer cell line), the best value was 1.42 µM [67], for the hybrid compound that is a part of the sandwich, C₂₅N₁₀Na_{0.7}Co_{5.3}O₇₆Sb₂W₁₈, and was the best result in this group of POMs.

On the other hand, on the BGC-823 cell line (human papillomavirus-related endocervical adenocarcinoma cell line), the best IC₅₀ was found at 48 h with the pure inorganic compound {Sb₈W₃₆} [67]. For the transformed human embryonic kidney cell line (HEK293T), the hybrid C₂₅N₁₀Na_{0.7}Co_{5.3}O₇₆Sb₂W₁₈ had the value of 103.09 µM at 48 h [67] and in the line OVCAR-3 (human ovarian cancer cell line), the best value was obtained at 72 h with POM [Co(H₂O)₆{CoSb₆O₄(H₂O)₃[Co(hmta)SbW₈O₃₁]₃}]¹³⁻ being 1.78 µM [66]. Comparing the effects of tungsten-containing POMs on the AGS, BGC-823 and HEK293T cell lines, studied at 48h, it was found that the POTs are more efficient (in ascending order) in the AGS (1.42 µM), BGC-823 (8.68 µM) and HEK293T (103.09 µM) [67]. Thus, compound 2 is 73-times more potent in the transformed human embryonic kidney cell line when compared to the human stomach cancer cell line. Relative to the first POM referred to, at 72 h, a 2-fold greater efficacy was observed in the human ovarian cancer cell line A2780 (0.77 µM), compared to OVCAR-3 (1.78 µM) [66]. It was also found in the A549 lineage (human lung tumor lines) that the most effective compound was [Co(H₂O)₆{CoSb₆O₄(H₂O)₃[Co(hmta)SbW₈O₃₁]₃}]¹³⁻ with a value of 12.75 µM [66] at 72 h, which was lower when compared to a value of 39.75 µM [67], found at 48 h, with the compound C₂₅N₁₀Na_{1.7}Ni_{5.3}O₈₂Sb₂W₁₈. However, as previously observed in studies where they tested at 24, 48 and 72 h (increasing incubation time), the IC₅₀ value tends to decrease.

In order to analyze whether antitumor drugs or POMs would be the most efficient, it was verified which drugs were tested in these strains and their respective IC₅₀ values (Table 3). In Table 3, the lowest value among the approved drugs was 14.85 µM in the U937 strain, at 24 h, using the drug ATRA. While in relation to compounds, the lower value belongs to NaB, being 1.20 µM in the DU145 strain, at 72 h, which is about 14-times lower than the lowest value of the tested drugs. As for the cell viability of medically approved drugs or compounds, only cell lines of human origin were used.

Table 3. IC₅₀ (μM) of the different antitumor drugs in the respective cell lines.

Compound	Cell Line	IC ₅₀ μM			Ref.
		24 h	48 h	72 h	
ATRA	HL-60	20.76			[60]
	U937	14.85			
Cisplatin	SH-SY5Y	28.40	11.60		[65]
	MG-63	43.00			[33]
	AGS		17.44		[67]
	BGC-823		5.78		
MTX	HepG2	42.03			[63]
	A549	26.93			
	MCF-7	49.79			
TSA	LNCaP			98.14	[68]
NaB				3.46	
TSA	DU145			59.45	
NaB				1.20	

When comparing the cell viability of clinically approved drugs and POMs, it was observed, for example, a value of 49.79 μM using the drug MTX [60] (Table 3), and a value of 1.53 μM using the compound VMOP-31 [59], in the MCF-7 strain (breast cancer cell line) at 24 h (Table 2). It was verified that the IC₅₀ value of the POM is lower, suggesting that the effects of POMs can overcome those of drugs. In fact, the dose necessary to have an inhibitory concentration of 50% is about 33-times lower than the dose that will be needed with a clinically approved drug.

Some drugs were tested in the strains mentioned above, such as ATRA (all-trans retinoid, also known as tretinoin), which is a drug used for the treatment of acne and acute promyelocytic leukemia (PML), having been tested in the HL-60 and U937 [60]. CDDP was tested on SH-SY5Y [65], MG-63 [33], AGS and BCG-823 [67] strains. The drug MTX (methotrexate), formerly known as amethopterin, a chemotherapeutic agent and immune system suppressor, used to treat cancer (cancer of the breast, leukemia, lung cancer, lymphoma, gestational trophoblastic disease and osteosarcoma), autoimmune diseases (i.e., psoriasis, rheumatoid arthritis and Crohn's disease) and in ectopic pregnancy and for medical abortions, was analyzed here in the lines HepG2, A549 and MCF-7 [63].

It was found with the drug ATRA that the lowest IC₅₀ value was 14.85 μM in the U937 strain, whereas a value of 20.76 μM was found in the HL-60 strain [60], both at 24 h. Cisplatin, at 24 h, is more effective in the SH-SY5Y strain (28.40 μM) [65], when compared to MG-63 (43.00 μM) [33]. On the other hand, at 48 h the lowest value was 5.78 μM in BCG-823 [67], conversely to the SH-SY5Y (11.60 μM) and AGS (17.44 μM) strains [67]. Finally, for the drug MTX at 24 h, the effect in the lines by order of increasing IC₅₀ were A549 (26.93 μM), HepG2 (42.03 μM) and MCF-7 (49.79 μM) [63].

When comparing TSA (trichostatin A, an organic compound that serves as an antifungal antibiotic and selectively inhibits the histone deacetylase (HDAC) enzyme families of class I and II mammals) with NaB, in the LNCaP and DU145 strains at 72 h, it is concluded that in both strains the NaB compound has the advantage, showing values of 3.46 and 1.20 μM, compared to 98.14 and 59.45 μM [68] for TSA, for the same strains. It was also found that the antitumor activity of V₁₈ was stronger than that of 5-Fu at 48 h for concentrations of 250 and 500 μM [58].

Moreover, taking in consideration the high IC₅₀ values for POMs at normal cells compared to cancer cells, it is established that these compounds showed *high selectivity towards* the cancer cell lines [69]. Therefore, POMs selectively target *cancer cells* while

sparing *healthy cells*, showing themselves to be promising agents in the treatment of cancer. In fact, POMs are expected to develop into the next generation of anticancer drugs [15,73].

2.3.2. Effect of POMs on the Cell Cycle

Similarly to the cell viability discussed above, the effects of POMs on the cell cycle were also discussed in all articles selected (Figure 5). Particularly within the effects of compounds on the cell cycle, we wanted to highlight where each one interrupts the cycle. In Figure 5, the percentage of numbers of articles in which each phase of the cell cycle stagnated was summarized, referring to each POM and lines in which they were tested. Table 4 shows a better precision of the action of POMs in the arrest of the cell cycle of the different lineages studied. It was also verified that there are lines in which, depending on the POM used, the cell cycle phase where they stop can be different, such as the SMMC-7721 and MCD-7 cell lines, which are in the G2/M phase and in the S phase, respectively. Globally, 56% of the POMs stopped the cell cycle in the S phase (red), which is during DNA synthesis, whereas 36% blocked the G2/M phase (green), that is, when the transition from interphase to onset of mitosis occurs. While the G1 phase is characteristic of the maturation in proteins and RNA (ribonucleic acid) synthesis, it was still only 8% of the POMs, namely in the compound $K_2Na[As^{III}Mo_6O_{21}(O_2CCH_2NH_3)_3]6H_2O$ [60], represented with the color yellow, that arrested the cell cycle at this stage. It is also verified that different POMs can stop the cell cycle in several phases (Figure 5).

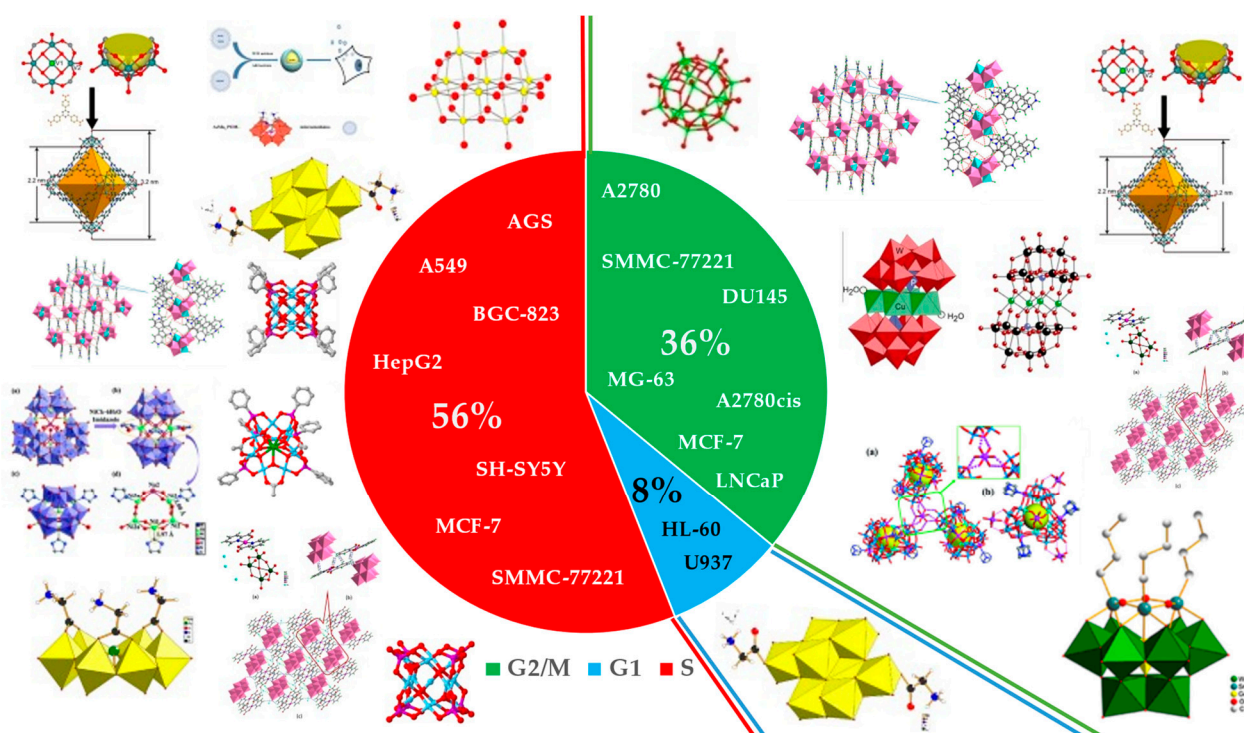


Figure 5. Percentage of the number of articles in which each cell cycle arrest occurred, referring to each POM used and respective cell lines. Color code: red—S phase [57,59,61–65,67]; green—G2/M [33,58,59,63,64,66,68] phase; and blue—G1 phase [60]. Reproduced from Refs. [63,66] with permission from the Royal Society of Chemistry. Reproduced from Refs. [33,57,60,62,71] with permission from Elsevier. Reproduced from Ref. [59] with permission from Wiley. Reproduced from Ref. [61] with permission from Plosone. Reproduced from Ref. [64] with permission from American Chemical Society. Reproduced from Ref. [65] with permission from Springer. Reproduced from Ref. [66] with permission from the Royal Society of Chemistry.

Table 4. Effect of POMs and their cell lines on cell cycle arrest.

Compound	Cell Line	Cell Cycle Arrest			Ref
		G1	S	G2/M	
POVs					
VMOP-31	SMMC-77221		✓	✓	[59]
CoV ₁₀	SMMC-77221		✓		[57]
V ₁₈	MCF-7			✓	[58]
POMos					
$K_2Na[As^{III}Mo_6O_{21}(O_2CCH_2NH_3)_3] \cdot 6H_2O - 1$	A549		✓		[62]
$K_2Na_2[\gamma-Mo_8O_{26}(O_2CCH_2NH_3)_2] - 2$	A549		✓		
[[4,4'-H ₂ bpy]{4,4'-Hbpy} ₂ {H ₂ P ₂ Mo ₅ O ₂₃ }] ₂ · 5H ₂ O	A549		✓		
	HepG2		✓		[63]
	MCF-7			✓	
[(Cu(pic) ₂) ₂ (Mo ₈ O ₂₆)] · 8H ₂ O	A549		✓		
	HepG2		✓		[64]
	MCF-7			✓	
$K_2Na[As^{III}Mo_6O_{21}(O_2CCH_2NH_3)_3] \cdot 6H_2O$	HL-60	✓			
	U937	✓			[60]
POM@SiO ₂	MCF-7		✓		[61]
POPds					
Pd ₁₃			✓		
Pd ₁₃ L	SH-SY5Y		✓		[65]
SrPd ₁₂			✓		
POTs					
[Co(H ₂ O) ₆ {CoSb ₆ O ₄ (H ₂ O) ₃ [Co(hmta)SbW ₈ O ₃₁] ₃ }] ¹³⁻ (1)	A2780			✓	
	A2780cis			✓	[66]
C25N10Na1.7Ni5.3O82Sb2W18—1	AGS		✓		
	BGC-823		✓		[67]
PAC-320	DU145			✓	
	LNCaP			✓	[68]
PW ₉ Cu	MG-63			✓	[33]

In order to analyze in detail which type of POM affected the different phases of the cell cycle in the respectively studied lines, a table was prepared, with the division of the phases of the cell cycle that were blocked by corresponding POMs and respective cell lines (Table 4).

It should be noted that in the articles where several POMs were studied, cell cycle arrest was only tested for the compound that showed the greatest efficacy. Likewise, of

the cell lines analyzed, only those that had presented the best efficacy values were focused on, to verify cell arrest. Therefore, in Table 4, when in relation to Table 2, we verified a smaller number of POMs and cell lines analyzed, namely, three POVs in two cell lines and six POMos in four lines, with the majority being the study of the A549 line, human lung cancer cell line. There were only three POPds for the neuroblastoma line (SH-SY5Y), and finally we found four POTs for seven cell lines, all distinct from each other (Table 4). As estimated, in these studies the concentrations at which compounds have an effect on the cell cycle are close or below the IC₅₀ previously determined and are described in Table 2.

As can be seen, the S phase is predominant under the action of the POMs with 14 of them, followed by the G2/M phase with nine polyoxometalates, and two in the G1 phase. It is also verified that VMOP-31 is the only one that has the ability to stop the cell cycle of SMMC-77221 cells in two distinct cell phases, namely S and G2/M [59]. On the other hand, it is also clear that the breast cancer cell line (MCF-7) on several compounds has its arrest in the G2/M phase, with the exception of the molybdenum compound involved in silica nanoparticles ($K_2Na[As^{III}Mo_6O_{21}(O_2CCH_2NH_3)_3] \cdot 6H_2O$ (POM@SiO₂)), stopping in the S phase [61].

Most of the proposed modes of action for antitumor POMs were recently reviewed [15]. Among these mechanisms, it was shown that POMs are able to affect DNA by interacting directly with it [15,58]. POMs were also suggested to cleave the phosphodiester bond and to affect DNA synthesis [15,74]. However, to our knowledge the processes responsible for the POMs effects that cause cell cycle arrest, as well as the effects in the cell cycle checkpoints, are unknown. For instance, the precise mechanism of action responsible for the POMs effects in DNA synthesis and/or in mitosis during the cell cycle process still needs to be deduced and needs further clarification.

3. Conclusions

In this review paper, bibliographic research was carried out with the keywords “polyoxometalates” AND “cell cycle”. Thirteen articles were selected on the effect of POMs with anticancer activities, namely in gastric, colon, liver, lung, ovary, breast, prostate, leukemia, osteosarcoma, neuroblastoma and human hepatocellular carcinoma. The types of cancer in which the articles most focused on were lung and breast cancer, with six articles each, followed by liver cancer, covered in four articles. The effects of POMs on cancer cells can be diverse, such as their interaction in the cell cycle, protein expression, mitochondrial effects, ROS production and cell viability. In the present study, we focused mainly on cell viability and cell cycle arrest, since all selected articles analyzed these two effects.

Cell viability was analyzed by dividing the POMs into sections according to the constituent compound, namely POVs, POMos, POPds and POTs. When the IC₅₀ values were compared and sorted in ascending order, it was found that the POV (VMOP-31) at 24, 48 and 72 h presented, respectively, the lowest values of 1.52, 0.63, and 0.53 μM, in the MCF-7 (human breast cancer cell line). In clinically approved drugs, the lowest IC₅₀ value was found to be 5.78 μM in the BCG-823 lineage at 48h using cisplatin. When comparing drugs and POMs, better results of POMs were observed. In many cases, the POMs dose required to have an inhibitory concentration of 50% is 2- to 200-times lower than the dose that would be necessary with a clinically approved drug. Therefore, POMs are future potential candidates for cancer therapeutic applications.

In addition to the cell viability, the effect of POMs on cell cycle arrest is highlighted. For the majority of the POMs, cell cycle arrest occurs mostly in the S phase (56%), where DNA synthesis occurs, whereas 36% blocks the G2/M phase. Fewer POMs interfere with the G1 phase (8%), that is, at the beginning of the cell cycle. Although the mechanism of action, directly and/or indirectly, responsible for the POMs cell cycle arrest is still to be deduced and clarified, the scientific evidence described above strengthens the potential use of such metallodrugs in anticancer therapy in the near future.

Author Contributions: Conceptualization, M.A.; Formal analysis, M.A.; Funding acquisition, M.A.; Investigation, F.C. and M.A.; Methodology, F.C. and M.A.; Supervision, M.A.; Writing–original draft, F.C. and M.A.; Writing–review & editing, F.C. and M.A. All authors have read and agreed to the published version of the manuscript.

Funding: This study received Portuguese national funds from FCT - Foundation for Science and Technology through projects UIDB/04326/2020, UIDP/04326/2020 and LA/P/0101/2020 (M.A.).

Institutional Review Board Statement: Not applicable.

Informed Consent Statement: Not applicable.

Data Availability Statement: The data is available in the original research papers.

Acknowledgments: The authors thanks to Neuza Fernandes and Rafael Polman for the English revision of the article.

Conflicts of Interest: The authors declare no conflict of interest.

Abbreviations

5-Fu	Fluorouracil
A2780	human ovarian cancer cell line
A2780cis	cisplatin-resistant human ovarian cancer cell line
A2780cisR	cisplatin-resistant human ovarian cancer cell line
A549	human lung cancer cell line
Ac	actinium
AGS	human stomach cancer cell line
As	arsenic
BEAS-2B	non-tumor human epithelial cell line of the bronchial epithelium
BGC-823	endocervical adenocarcinoma cell line related to human papillomavirus
Co	cobalt
CoV ₁₀	Na ₄ Co ₆ V ₁₀ O ₂₈ ·18H ₂ O
CT26	murine colorectal carcinoma cell line that is from a BALB/c mouse.
CDDP	cisplatin or cis-diamminedichloroplatinum(II)
CDK	cyclin dependent kinase
CDKN2A	cyclin-dependent kinase inhibitor 2A
DHE	dihydroethidium
DHR-123	dihydrorhodamine-123 oxidation test
DNA	deoxyribonucleic acid
DU145	human prostate cancer cell line
ΔΨ _m	mitochondrial membrane potential
<i>E. coli</i>	<i>Escherichia coli</i>
H1299	non-small cell lung carcinoma human cell line
H22	hepatoma-22, Mouse liver tumor cell line
HDACI	histone Deacetylase Inhibitor
Hep-A-22	mouse liver cancer lineage
HEK-293T	transformed human embryonic kidney cell line
HepG2	human hepatocarcinoma cell line
HL-60	human leukemia cell line
HPOMs	heteropolyoxometalates
HT29	human colon adenocarcinoma cell line
HUVEC	human umbilical vein endothelial cells
IC ₅₀	50% inhibitory concentration
LNCaP	androgen-sensitive prostate adenocarcinoma human cell line
MC3T3-E1	osteoblast precursor cell line sub-line derived from <i>Mus musculus</i> (Mouse) calvaria
MCF-7	human breast cancer cell line

MDA-MB-231	human breast cancer epithelial cell lineage
MG-63	cell that has fibroblast morphology isolated from the bone of a patient with osteosarcoma
MMP	mitochondrial membrane potential
Mn	manganese
Mo	molybdenum
MoO ₄ ²⁻	molybdate
Na	sodium
NaB	sodium butyrate
Nb	niobium
O ₂ ⁻	anion superoxide
OVCAR-3	human ovarian cancer cell line
P	phosphor
PAC-320	{(n-Bu)Sn(OH)} ₃ GeW ₉ O ₃₄] ⁴⁻ ·26H ₂ O
PbPd ₁₂	Na ₁₂ [Pb ^{IV} O ₈ Pd ₁₂ (PO ₄) ₈]·38H ₂ O
Pd ₁₃	Na ₈ [Pd ₁₃ As ₈ O ₃₄ (OH) ₆]·42H ₂ O
Pd ₁₃ L	Na ₆ [Pd ₁₃ (PhAsO ₃) ₈]·23H ₂ O
POM	polyoxometalate
POM@Sio2	K ₂ Na[As ^{III} Mo ₆ O ₂₁ (O ₂ CCH ₂ NH ₃) ₃]·6H ₂ O
POMs	polyoxometalates
POMos	polyoxomolybdates
PONMs	noble polyoxo metalates
POPs	polyoxopaladates
POVs	polyoxovanadates
POTs	polyoxotungstates
PS	phosphatidylserine
PW9Cu	K ₇ Na ₃ [Cu ₄ (H ₂ O) ₂ (PW ₉ O ₃₄) ₂]20H ₂ O
ROS	oxigen-reactive species
SAHA	suberoylanilide acid—Vorinostat
SARS-CoV	severe acute respiratory syndrome coronavirus
SH-SY5Y	subline cloned three times from neuroblastoma cell line SK-N-SH (ATCC HTB-11)
SK-OV-3	ovarian cancer human epithelial cell line
SMMC-7721	endocervical adenocarcinoma cell line related to human papillomavirus
SnPd ₁₂	Na ₁₂ [Sn ^{IV} O ₈ Pd ₁₂ (PO ₄) ₈]·43H ₂ O
SrPd ₁₂	Na ₄ [SrPd ₁₂ O ₆ (OH) ₃ (PhAsO ₃) ₆ (OAc) ₃] 2NaOAc·32H ₂ O
Ta	tantalum
Tc	technetium
U937	histiocytic lymphoma human cell line
UMR106	epithelial cell isolated from the bone of a mouse with osteosarcoma
V	vanadium
V ₁₈	K ₁₂ [V ₁₈ O ₄₂ (H ₂ O)] 6H ₂ O
VMOP-31	6{V ₅ O ₉ Cl(COO) ₄ }
W	tungsten

References

- Peña, Q.; Wang, A.; Zaremba, O.; Shi, Y.; Scheeren, H.W.; Metselaar, J.M.; Kiessling, F.; Pallares, R.M.; Wuttke, S.; Lammers, T. Metallodrugs in Cancer Nanomedicine. *Chem. Soc. Rev.* **2022**, *51*, 2544–2582. [[CrossRef](#)] [[PubMed](#)]
- Ochoa, E.L.M. Lithium as a Neuroprotective Agent for Bipolar Disorder: An Overview. *Cell. Mol. Neurobiol.* **2022**, *42*, 85–97. [[CrossRef](#)] [[PubMed](#)]
- Vosahlikova, M.; Roubalova, L.; Cechova, K.; Kaufman, J.; Musil, S.; Miksik, I.; Alda, M.; Svoboda, P. Na⁺/K⁺-ATPase and Lipid Peroxidation in Forebrain Cortex and Hippocampus of Sleep-Deprived Rats Treated with Therapeutic Lithium Concentration for Different Periods of Time. *Prog. Neuropsychopharmacol. Biol. Psychiatry* **2020**, *102*, 109953. [[CrossRef](#)] [[PubMed](#)]
- Bertinat, R.; Westermeier, F.; Gatica, R.; Nualart, F. Sodium Tungstate: Is It a Safe Option for a Chronic Disease Setting, Such as Diabetes? *J. Cell. Physiol.* **2019**, *234*, 51–60. [[CrossRef](#)] [[PubMed](#)]
- Silva, M.J.S.A.; Gois, P.M.P.; Gasser, G. Unveiling the Potential of Transition Metal Complexes for Medicine: Translational *in Situ* Activation of Metal-Based Drugs from Bench to *in Vivo* Applications. *ChemBioChem* **2021**, *22*, 1740–1742. [[CrossRef](#)]

6. Ścibior, A.; Pietrzyk, Ł.; Plewa, Z.; Skiba, A. Vanadium: Risks and Possible Benefits in the Light of a Comprehensive Overview of Its Pharmacotoxicological Mechanisms and Multi-Applications with a Summary of Further Research Trends. *J. Trace. Elem. Med. Biol.* **2020**, *61*, 126508. [[CrossRef](#)]
7. Yeo, C.; Ooi, K.; Tiekink, E. Gold-Based Medicine: A Paradigm Shift in Anti-Cancer Therapy? *Molecules* **2018**, *23*, 1410. [[CrossRef](#)]
8. Soria-Carrera, H.; Atrián-Blasco, E.; de la Fuente, J.M.; Mitchell, S.G.; Martín-Rapún, R. Polyoxometalate–Polypeptide Nanoassemblies as Peroxidase Surrogates with Antibiofilm Properties. *Nanoscale* **2022**, *14*, 5999–6006. [[CrossRef](#)]
9. Soria-Carrera, H.; Franco-Castillo, I.; Romero, P.; Martín, S.; Fuente, J.M.; Mitchell, S.G.; Martín-Rapún, R. On-POM Ring-Opening Polymerisation of *N*-Carboxyanhydrides. *Angew. Chem. Int. Ed. Engl.* **2021**, *60*, 3449–3453. [[CrossRef](#)]
10. Aureliano, M.; Marques-da-Silva, D.; Serrano, A.; Martins, J.; Faleiro, L.; Fonseca, C.; Fraqueza, G.; Lagoa, R. Chapter 7, Polyoxometalates with anticancer, antibacterial and antiviral activities. In *Polyoxometalates: Advances, Properties, and Applications*, 1st ed.; Rubio, L.R., Artetxe, B., Gutiérrez-Zorrilla, J.M., Vilas, J.L., Eds.; Jenny Stanford Publishing: Singapore, 2022; ISBN 9781003277446/9789814968140.
11. Pimpão, C.; da Silva, I.V.; Mósca, A.F.; Pinho, J.O.; Gaspar, M.M.; Gumerova, N.I.; Rompel, A.; Aureliano, M.; Soveral, G. The Aquaporin-3-Inhibiting Potential of Polyoxotungstates. *Int. J. Mol. Sci.* **2020**, *21*, 2467. [[CrossRef](#)]
12. Gumerova, N.; Krivosudský, L.; Fraqueza, G.; Breibeck, J.; Al-Sayed, E.; Tanuhadi, E.; Bijelic, A.; Fuentes, J.; Aureliano, M.; Rompel, A. The P-Type ATPase Inhibiting Potential of Polyoxotungstates. *Metallomics* **2018**, *10*, 287–295. [[CrossRef](#)] [[PubMed](#)]
13. Fraqueza, G.; Fuentes, J.; Krivosudský, L.; Dutta, S.; Mal, S.S.; Roller, A.; Giester, G.; Rompel, A.; Aureliano, M. Inhibition of Na⁺/K⁺- and Ca²⁺-ATPase Activities by Phosphotetradecavanadate. *J. Inorg. Biochem.* **2019**, *197*, 110700. [[CrossRef](#)] [[PubMed](#)]
14. Aureliano, M.; Fraqueza, G.; Berrocal, M.; Cordoba-Granados, J.J.; Gumerova, N.I.; Rompel, A.; Gutierrez-Merino, C.; Mata, A.M. Inhibition of SERCA and PMCA Ca²⁺-ATPase Activities by Polyoxotungstates. *J. Inorg. Biochem.* **2022**, *236*, 111952. [[CrossRef](#)] [[PubMed](#)]
15. Bijelic, A.; Aureliano, M.; Rompel, A. Polyoxometalates as Potential Next-Generation Metallodrugs in the Combat Against Cancer. *Angew. Chem. Int. Ed. Engl.* **2019**, *58*, 2980–2999. [[CrossRef](#)]
16. Bijelic, A.; Aureliano, M.; Rompel, A. The Antibacterial Activity of Polyoxometalates: Structures, Antibiotic Effects and Future Perspectives. *Chem. Comm.* **2018**, *54*, 1153–1169. [[CrossRef](#)]
17. Čolović, M.B.; Lacković, M.; Lalatović, J.; Mougharbel, A.S.; Kortz, U.; Krstić, D.Z. Polyoxometalates in Biomedicine: Update and Overview. *Curr. Med. Chem.* **2020**, *27*, 362–379. [[CrossRef](#)]
18. Aureliano, M.; Gumerova, N.I.; Sciortino, G.; Garribba, E.; Rompel, A.; Crans, D.C. Polyoxovanadates with Emerging Biomedical Activities. *Coord. Chem. Rev.* **2021**, *447*, 214143. [[CrossRef](#)]
19. Aureliano, M.; Gumerova, N.I.; Sciortino, G.; Garribba, E.; McLauchlan, C.C.; Rompel, A.; Crans, D.C. Polyoxidovanadates' Interactions with Proteins: An Overview. *Coord. Chem. Rev.* **2022**, *454*, 214344. [[CrossRef](#)]
20. Guedes, G.; Wang, S.; Santos, H.A.; Sousa, F.L. Polyoxometalate Composites in Cancer Therapy and Diagnostics. *Eur. J. Inorg. Chem.* **2020**, *2020*, 2121–2132. [[CrossRef](#)]
21. Aureliano, M. The Future Is Bright for Polyoxometalates. *BioChem* **2022**, *2*, 8–26. [[CrossRef](#)]
22. Aureliano, M. Decavanadate: A Journey in a Search of a Role. *Dalton Trans.* **2009**, 9093. [[CrossRef](#)] [[PubMed](#)]
23. Aureliano, M.; Fraqueza, G.; Ohlin, C.A. Ion Pumps as Biological Targets for Decavanadate. *Dalton Trans.* **2013**, *42*, 11770. [[CrossRef](#)]
24. Crans, D.C.; Smee, J.J.; Gaidamauskas, E.; Yang, L. The Chemistry and Biochemistry of Vanadium and the Biological Activities Exerted by Vanadium Compounds. *Chem. Rev.* **2004**, *104*, 849–902. [[CrossRef](#)] [[PubMed](#)]
25. Aureliano, M.; Crans, D.C. Decavanadate (V10O286-) and Oxovanadates: Oxometalates with Many Biological Activities. *J. Inorg. Biochem.* **2009**, *103*, 536–546. [[CrossRef](#)] [[PubMed](#)]
26. Sciortino, G.; Aureliano, M.; Garribba, E. Rationalizing the Decavanadate(V) and Oxidovanadium(IV) Binding to G-Actin and the Competition with Decaniobate(V) and ATP. *Inorg. Chem.* **2021**, *60*, 334–344. [[CrossRef](#)]
27. Treviño, S.; Díaz, A.; Sánchez-Lara, E.; Sanchez-Gaytan, B.L.; Perez-Aguilar, J.M.; González-Vergara, E. Vanadium in Biological Action: Chemical, Pharmacological Aspects, and Metabolic Implications in Diabetes Mellitus. *Biol. Trace Elem. Res.* **2019**, *188*, 68–98. [[CrossRef](#)]
28. Treviño, S.; González-Vergara, E. Metformin-Decavanadate Treatment Ameliorates Hyperglycemia and Redox Balance of the Liver and Muscle in a Rat Model of Alloxan-Induced Diabetes. *New J. Chem.* **2019**, *43*, 17850–17862. [[CrossRef](#)]
29. Treviño, S.; Velázquez-Vázquez, D.; Sánchez-Lara, E.; Diaz-Fonseca, A.; Flores-Hernandez, J.Á.; Pérez-Benítez, A.; Brambila-Colombres, E.; González-Vergara, E. Metforminium Decavanadate as a Potential Metallopharmaceutical Drug for the Treatment of Diabetes Mellitus. *Oxid. Med. Cell. Longev.* **2016**, *2016*, 6058705. [[CrossRef](#)]
30. Sánchez-Lombardo, I.; Sánchez-Lara, E.; Pérez-Benítez, A.; Mendoza, Á.; Bernès, S.; González-Vergara, E. Synthesis of Metforminium(2+) Decavanadates—Crystal Structures and Solid-State Characterization. *Eur. J. Inorg. Chem.* **2014**, *2014*, 4581–4588. [[CrossRef](#)]
31. Chatkon, A.; Chatterjee, P.B.; Sedgwick, M.A.; Haller, K.J.; Crans, D.C. Counterion Affects Interaction with Interfaces: The Antidiabetic Drugs Metformin and Decavanadate. *Eur. J. Inorg. Chem.* **2013**, *2013*, 1859–1868. [[CrossRef](#)]
32. Sánchez-Lara, E.; Treviño, S.; Sánchez-Gaytán, B.L.; Sánchez-Mora, E.; Eugenia Castro, M.; Meléndez-Bustamante, F.J.; Méndez-Rojas, M.A.; González-Vergara, E. Decavanadate Salts of Cytosine and Metformin: A Combined Experimental-Theoretical Study of Potential Metallodrugs against Diabetes and Cancer. *Front. Chem.* **2018**, *6*, 402. [[CrossRef](#)] [[PubMed](#)]

33. León, I.E.; Porro, V.; Astrada, S.; Egusquiza, M.G.; Cabello, C.I.; Bollati-Fogolin, M.; Etcheverry, S.B. Polyoxometalates as Antitumor Agents: Bioactivity of a New Polyoxometalate with Copper on a Human Osteosarcoma Model. *Chem. Biol. Interact.* **2014**, *222*, 87–96. [[CrossRef](#)] [[PubMed](#)]
34. Yamase, T. Polyoxometalates Active against Tumors, Viruses, and Bacteria. *Prog. Mol. Subcell. Biol.* **2013**, *54*, 65–116. [[CrossRef](#)] [[PubMed](#)]
35. Van Rompuy, L.S.; Parac-Vogt, T.N. Interactions between Polyoxometalates and Biological Systems: From Drug Design to Artificial Enzymes. *Curr. Opin. Biotechnol.* **2019**, *58*, 92–99. [[CrossRef](#)] [[PubMed](#)]
36. Wang, S.; Sun, W.; Hu, Q.; Yan, H.; Zeng, Y. Synthesis and Evaluation of Pyridinium Polyoxometalates as Anti-HIV-1 Agents. *Bioorg. Med. Chem. Lett.* **2017**, *27*, 2357–2359. [[CrossRef](#)]
37. Francese, R.; Civra, A.; Rittà, M.; Donalizio, M.; Argenziano, M.; Cavalli, R.; Mougharbel, A.S.; Kortz, U.; Lembo, D. Anti-Zika Virus Activity of Polyoxometalates. *Antiviral. Res.* **2019**, *163*, 29–33. [[CrossRef](#)] [[PubMed](#)]
38. Enderle, A.G.; Bosso, M.; Groß, R.; Heiland, M.; Bollini, M.; Culzoni, M.J.; Kirchhoff, F.; Münch, J.; Streb, C. Increased in Vitro Anti-HIV Activity of Caffeinium-Functionalized Polyoxometalates. *ChemMedChem* **2021**, *16*, 2727–2730. [[CrossRef](#)] [[PubMed](#)]
39. Shahabadi, N.; Mahdavi, M.; Zندهcheshm, S. Can Polyoxometalates (POMs) Prevent of Coronavirus 2019-NCov Cell Entry? Interaction of POMs with TMPRSS2 and Spike Receptor Domain Complexed with ACE2 (ACE2-RBD): Virtual Screening Approaches. *Inform. Med. Unlocked* **2022**, *29*, 100902. [[CrossRef](#)] [[PubMed](#)]
40. Raza, R.; Matin, A.; Sarwar, S.; Barsukova-Stuckart, M.; Ibrahim, M.; Kortz, U.; Iqbal, J. Polyoxometalates as Potent and Selective Inhibitors of Alkaline Phosphatases with Profound Anticancer and Amoebicidal Activities. *Dalton Trans.* **2012**, *41*, 14329. [[CrossRef](#)] [[PubMed](#)]
41. Liu, J.C.; Wang, J.F.; Han, Q.; Shanguan, P.; Liu, L.L.; Chen, L.J.; Zhao, J.W.; Streb, C.; Song, Y.F. Multicomponent Self-Assembly of a Giant Heterometallic Polyoxotungstate Supercluster with Antitumor Activity. *Angew. Chem. Int. Ed. Engl.* **2021**, *60*, 11153–11157. [[CrossRef](#)] [[PubMed](#)]
42. Fu, L.; Gao, H.; Yan, M.; Li, S.; Li, X.; Dai, Z.; Liu, S. Polyoxometalate-Based Organic-Inorganic Hybrids as Antitumor Drugs. *Small* **2015**, *11*, 2938–2945. [[CrossRef](#)] [[PubMed](#)]
43. Zheng, W.; Yang, L.; Liu, Y.; Qin, X.; Zhou, Y.; Zhou, Y.; Liu, J. Mo Polyoxometalate Nanoparticles Inhibit Tumor Growth and Vascular Endothelial Growth Factor Induced Angiogenesis. *Sci. Technol. Adv. Mater.* **2014**, *15*, 035010. [[CrossRef](#)] [[PubMed](#)]
44. Boulmier, A.; Feng, X.; Oms, O.; Mialane, P.; Rivière, E.; Shin, C.J.; Yao, J.; Kubo, T.; Furuta, T.; Oldfield, E.; et al. Anticancer Activity of Polyoxometalate-Bisphosphonate Complexes: Synthesis, Characterization, in Vitro and in Vivo Results. *Inorg. Chem.* **2017**, *56*, 7558–7565. [[CrossRef](#)]
45. Li, D.; Gao, X.; Gu, J.; Tian, Y.; Liu, Y.; Jin, Z.; Yan, D.; Chen, Y.G.; Zhu, X. A Novel Application of Ti-Substituted Polyoxometalates: Anti-Inflammatory Activity in OVA-Induced Asthma Murine Model. *Bioinorg. Chem. Appl.* **2016**, *2016*, 3239494. [[CrossRef](#)] [[PubMed](#)]
46. Zhang, S.; Li, M.; Zhang, Y.; Wang, R.; Song, Y.; Zhao, W.; Lin, S. A Supramolecular Complex Based on a Gd-Containing Polyoxometalate and Food-Borne Peptide for MRI/CT Imaging and NIR-Triggered Photothermal Therapy. *Dalton Trans.* **2021**, *50*, 8076–8083. [[CrossRef](#)]
47. Pérez-Álvarez, L.; Ruiz-Rubio, L.; Artetxe, B.; Vivanco, M.d.M.; Gutiérrez-Zorrilla, J.M.; Vilas-Vilela, J.L. Chitosan Nanogels as Nanocarriers of Polyoxometalates for Breast Cancer Therapies. *Carbohydr. Polym.* **2019**, *213*, 159–167. [[CrossRef](#)]
48. Ma, M.; Gao, N.; Sun, Y.; Du, X.; Ren, J.; Qu, X. Redox-Activated Near-Infrared-Responsive Polyoxometalates Used for Photothermal Treatment of Alzheimer's Disease. *Adv. Healthc. Mater.* **2018**, *7*, 1800320. [[CrossRef](#)]
49. Li, M.; Guan, Y.; Zhao, A.; Ren, J.; Qu, X. Using Multifunctional Peptide Conjugated Au Nanorods for Monitoring β -Amyloid Aggregation and Chemo-Photothermal Treatment of Alzheimer's Disease. *Theranostics* **2017**, *7*, 2996–3006. [[CrossRef](#)]
50. Gao, N.; Sun, H.; Dong, K.; Ren, J.; Duan, T.; Xu, C.; Qu, X. Transition-Metal-Substituted Polyoxometalate Derivatives as Functional Anti-Amyloid Agents for Alzheimer's Disease. *Nat. Commun.* **2014**, *5*, 3422. [[CrossRef](#)]
51. Bălăci, Ș.; Șuşman, S.; Rusu, D.; Nicula, G.Z.; Sorițău, O.; Rusu, M.; Biris, A.S.; Matei, H. Differentiation of Stem Cells into Insulin-Producing Cells under the Influence of Nanostructural Polyoxometalates. *J. Appl. Toxicol.* **2016**, *36*, 373–384. [[CrossRef](#)]
52. Amante, C.; De Sousa-Coelho, A.L.; Aureliano, M. Vanadium and Melanoma: A Systematic Review. *Metals* **2021**, *11*, 828. [[CrossRef](#)]
53. Fonseca, C.; Aureliano, M. Biological Activity of Gold Compounds against Viruses and Parasitosis: A Systematic Review. *BioChem* **2022**, *2*, 145–159. [[CrossRef](#)]
54. Aureliano, M.; Mitchell, S.G.; Yin, P. Editorial: Emerging polyoxometalates with biological, biomedical, and health applications. *Front. Chem.* **2022**, *10*, 977317. [[CrossRef](#)] [[PubMed](#)]
55. De Sousa-Coelho, A.L.; Aureliano, M.; Fraqueza, G.; Serrao, G.; Goncalves, J.; Sanchez-Lombardo, I.; Link, W.; Ferreira, B.I. Decavanadate and metformin-decavanadate effects in human melanoma cells. *J. Inorg. Biochem.* **2022**, *235*, 111915. [[CrossRef](#)]
56. Faleiro, L.; Marques, A.; Martins, J.; Jordão, L.; Nogueira, I.; Gumerova, N.I.; Rompel, A.; Aureliano, M. The Preyssler-Type Polyoxotungstate Exhibits Anti-Quorum Sensing, Antibiofilm, and Antiviral Activities. *Biology* **2022**, *11*, 994. [[CrossRef](#)]
57. Zhai, F.; Wang, X.; Li, D.; Zhang, H.; Li, R.; Song, L. Synthesis and Biological Evaluation of Decavanadate $\text{Na}_4\text{Co}(\text{H}_2\text{O})_6\text{V}_{10}\text{O}_{28}\cdot 18\text{H}_2\text{O}$. *Biomed. Pharmacother.* **2009**, *63*, 51–55. [[CrossRef](#)]
58. Qi, W.; Zhang, B.; Qi, Y.; Guo, S.; Tian, R.; Sun, J.; Zhao, M. The Anti-Proliferation Activity and Mechanism of Action of $\text{K}_{12}[\text{V}_{18}\text{O}_{42}(\text{H}_2\text{O})_6]\cdot 6\text{H}_2\text{O}$ on Breast Cancer Cell Lines. *Molecules* **2017**, *22*, 1535. [[CrossRef](#)]

59. Zheng, Y.; Gan, H.; Zhao, Y.; Li, W.; Wu, Y.; Yan, X.; Wang, Y.; Li, J.; Li, J.; Wang, X. Self-Assembly and Antitumor Activity of a Polyoxovanadate-Based Coordination Nanocage. *Chem-Eur. J.* **2019**, *25*, 15326–15332. [[CrossRef](#)]
60. Li, C.; Cao, H.; Sun, J.; Tian, R.; Li, D.; Qi, Y.; Yang, W.; Li, J. Antileukemic Activity of an Arsenomolybdate in the Human HL-60 and U937 Leukemia Cells. *J. Inorg. Biochem.* **2017**, *168*, 67–75. [[CrossRef](#)]
61. Cao, H.; Li, C.; Qi, W.; Meng, X.; Tian, R.; Qi, Y.; Yang, W.; Li, J. Synthesis, Cytotoxicity and Antitumor Mechanism Investigations of Polyoxometalate Doped Silica Nanospheres on Breast Cancer MCF-7 Cells. *PLoS ONE* **2017**, *12*, e0181018. [[CrossRef](#)]
62. Li, C.; Qi, W.; Cao, H.; Qi, Y.; Zhang, S.; Xu, S.; Sun, J.; Guo, S. BSA-Binding Properties and Anti-Proliferative Effects of Amino Acids Functionalized Polyoxomolybdates. *Biomed. Pharmacother.* **2016**, *79*, 78–86. [[CrossRef](#)] [[PubMed](#)]
63. Joshi, A.; Gupta, R.; Singh, B.; Sharma, D.; Singh, M. Effective Inhibitory Activity against MCF-7, A549 and HepG2 Cancer Cells by a Phosphomolybdate Based Hybrid Solid. *Dalton Trans.* **2020**, *49*, 7069–7077. [[CrossRef](#)] [[PubMed](#)]
64. Joshi, A.; Gupta, R.; Vaghasiya, K.; Verma, R.K.; Sharma, D.; Singh, M. In Vitro Anti-Tumoral and Anti-Bacterial Activity of an Octamolybdate Cluster-Based Hybrid Solid Incorporated with a Copper Picolinate Complex. *ACS Appl. Bio. Mater.* **2020**, *3*, 4025–4035. [[CrossRef](#)] [[PubMed](#)]
65. Isakovic, A.M.; Čolović, M.B.; Ma, T.; Ma, X.; Jeremic, M.; Gerić, M.; Gajski, G.; Misirlic-Dencic, S.; Kortz, U.; Krstić, D. Selected Polyoxopalladates as Promising and Selective Antitumor Drug Candidates. *J. Biol. Inorg. Chem.* **2021**, *26*, 957–971. [[CrossRef](#)] [[PubMed](#)]
66. Zhang, Z.M.; Duan, X.; Yao, S.; Wang, Z.; Lin, Z.; Li, Y.G.; Long, L.S.; Wang, E.B.; Lin, W. Cation-Mediated Optical Resolution and Anticancer Activity of Chiral Polyoxometalates Built from Entirely Achiral Building Blocks. *Chem. Sci.* **2016**, *7*, 4220–4229. [[CrossRef](#)] [[PubMed](#)]
67. Zhao, H.; Tao, L.; Zhang, F.; Zhang, Y.; Liu, Y.; Xu, H.; Diao, G.; Ni, L. Transition Metal Substituted Sandwich-Type Polyoxometalates with a Strong Metal-C (Imidazole) Bond as Anticancer Agents. *Chem. Commun.* **2019**, *55*, 1096–1099; Correction in *Chem. Commun.* **2020**, *56*, 2364.
68. Dong, Z.; Yang, Y.; Liu, S.; Lu, J.; Huang, B.; Zhang, Y. HDAC Inhibitor PAC-320 Induces G2/M Cell Cycle Arrest and Apoptosis in Human Prostate Cancer. *Oncotarget* **2018**, *9*, 512–523. [[CrossRef](#)]
69. Dong, Z.; Tan, R.; Cao, J.; Yang, Y.; Kong, C.; Du, J.; Zhu, S.; Zhang, Y.; Lu, J.; Huang, B.; et al. Discovery of Polyoxometalate-Based HDAC Inhibitors with Profound Anticancer Activity in Vitro and in Vivo. *Eur. J. Med. Chem.* **2011**, *46*, 2477–2484. [[CrossRef](#)]
70. Mann, B.S.; Johnson, J.R.; Cohen, M.H.; Justice, R.; Pazdur, R. FDA Approval Summary: Vorinostat for Treatment of Advanced Primary Cutaneous T-Cell Lymphoma. *Oncologist* **2007**, *12*, 1247–1252. [[CrossRef](#)]
71. Wang, X.; Wei, S.; Zhao, C.; Li, X.; Jin, J.; Shi, X.; Su, Z.; Li, J.; Wang, J. Promising application of polyoxometalates in the treatment of cancer, infectious diseases and Alzheimer's disease. *J. Biol. Inorg. Chem.* **2022**, *27*, 405–419. [[CrossRef](#)] [[PubMed](#)]
72. Qu, X.; Xu, K.; Zhao, C.; Song, X.; Li, J.; Li, L.; Nie, W.; Bao, H.; Wang, J.; Niu, F.; et al. Genotoxicity and acute and subchronic toxicity studies of a bioactive polyoxometalate in Wistar rats. *BMC Pharmacol. Toxicol.* **2017**, *18*, 26. [[CrossRef](#)] [[PubMed](#)]
73. Dinčić, M.; Čolović, M.B.; Sarić Matutinović, M.; Četković, M.; Kravić Stevović, T.; Mougharbel, A.S.; Todorović, J.; Ignjatović, S.; Radosavljević, B.; Milisavljević, M.; et al. *In vivo* toxicity evaluation of two polyoxotungstates with potential antidiabetic activity using Wistar rats as a model system. *RSC Adv.* **2020**, *10*, 2846–2855. [[CrossRef](#)] [[PubMed](#)]
74. Steens, N.; Ramadan, A.M.; Absillis, G.; Parac-Vogt, T.N. Hydrolytic cleavage of DNA-model substrates promoted by polyoxidoanadates. *Dalton Trans.* **2010**, *39*, 585–592. [[CrossRef](#)]

Disclaimer/Publisher's Note: The statements, opinions and data contained in all publications are solely those of the individual author(s) and contributor(s) and not of MDPI and/or the editor(s). MDPI and/or the editor(s) disclaim responsibility for any injury to people or property resulting from any ideas, methods, instructions or products referred to in the content.